Generation of Single-Walled Carbon Nanotubes from Alcohol and Generation Mechanism by Molecular Dynamics Simulations

Shigeo Maruyama, Yoichi Murakami, Yasushi Shibuta, Yuhei Miyauchi, and Shohei Chiashi

Corresponding Author: Shigeo Maruyama

Department of Mechanical Engineering, The University of Tokyo

7-3-1 Hongo, Bunkyo-ku, Tokyo 113-8656, Japan

TEL: +81-3-5841-6421, FAX: +81-3-5800-6983

E-Mail: maruyama@photon.t.u-tokyo.ac.jp

Abstract

Recent advances in high-purity and high-yield catalytic CVD generation of single-walled carbon nanotubes (SWNTs) from alcohol are comprehensively presented and discussed based on the results obtained from both experimental and numerical investigations. We have uniquely adopted alcohol as a carbon feedstock and this has resulted in high quality, low temperature synthesis of SWNTs. This technique can produce SWNTs even at a very low temperature of 550 °C that is about 300 °C lower than the conventional CVD methods where methane or acetylene are typically employed. The proposed alcohol CCVD method demonstrates its excellence in high yield production of SWNTs when Fe/Co on USY-zeolite powder was employed as a catalyst. At an optimum CVD condition, the SWNT yield of more than 40 wt% was achieved over the weight of the catalytic powder within the reaction time of 120 min. In addition to the advantages in mass production, this method is also suitable for the direct synthesis of high-quality SWNTs on Si and quartz substrates when combined with newly developed liquid-based 'dip-coat' technique to mount catalytic metals on the surface of substrates. This method allows an easy and costless loading of catalytic metals without necessitating any support or underlayer materials that were usually required in the past studies for the generation of SWNTs with sufficient quality on Si surface. Finally, the result of molecular dynamics simulation for the SWNT growth process is presented to obtain a fundamental insight of initial growth mechanism on the catalytic particles.

Keywords -

Single-Walled Carbon Nanotubes, CVD, Alcohol, Molecular Dynamics Method, Growth Mechanism

1. Introduction

Developments of large scale and high-purity generation technique of single-walled carbon nanotubes (SWNTs) [1] are desired for the practical applications of this fascinating new material. In addition to previously known laser-furnace [2] and arc-discharge [3] techniques, various catalytic chemical vapor deposition (CCVD) methods [4] have been proposed for the possible larger amount production with lower cost. At present, so-called HiPco process [5, 6] using floated catalyst during CVD process is known as one of the commercially feasible method for the mass production of SWNTs. Besides the floated catalyst approach, several studies that employed metal support material have been reported so far [7-15]. However, according to their TEM pictures [5, 6, 10, 12-15], they often suffer from the mixing of metal particles and amorphous carbon impurities among the produced SWNTs, and therefore the very best approach has not been found for achieving both the quality and yield simultaneously.

As one possible approach, we proposed a catalytic CVD technique using alcohol as a carbon source [16, 17], which can be performed at significantly low temperature around 600 °C with assuring as-prepared high-quality [16]. In the first part of this report, we present the feature of proposed alcohol catalytic CVD (ACCVD) technique to demonstrate the feasibility of our SWNTs toward mass production. The characterization of thereby synthesized as-grown SWNTs was performed by Raman, TGA, and TEM analyses for the discussion of the quality and yield. In addition to the bulk amount synthesis of SWNTs, we have developed a technique of synthesizing high-quality SWNTs directly on the surface of silicon and quartz substrates [18]. We also have attempted spatially controlled growth of SWNTs using SBA-16 type mesoporous silica (MPS) thin films coated on a Si substrate as a template for the SWNT growth [19]. These are presented and discussed in the later section of this report.

In order for the further optimization of SWNT generation process, understanding of the formation mechanism is really essential. It is especially critical for the future development of SWNT synthesis techniques with controlled diameter and chirality. In the end of this report, the nucleation and growth process of SWNTs were studied with classical molecular dynamics simulations. Specifically, we started from an initial state where carbon atoms were randomly allocated along with catalytic metal atoms, the nucleation processes of SWNTs were simulated and discussed both for the laser-furnace and CCVD situations.

2. CVD apparatus and procedure

Figure 1 shows the schematic of our ACCVD apparatus that is composed of an ethanol reservoir placed in a hot water bath, a quartz tube of 26 mm inner diameter and 1 m length, an electric furnace of 30 cm length, and a rotary pump to evacuate inside of the quartz tube. The quartz tube and rotary pump were connected via two paths, which are main-drain tube and sub-drain tube to adjust the pumping rate. The sample to undergo the CVD reaction is placed on a quartz boat, which is located in the central position of the quartz tube. Depending on the experiment, either Ar or Ar/H_2 (3% H_2) was flowed while heating-up of the electric furnace with only the sub-drain path kept open so that the inside of the quartz tube was maintained around 300 Torr. The use of H_2 is for the purpose of pre-reduction of the catalytic metals, which would be otherwise slowly reduced by alcohol during the CVD reaction. After the desired reaction temperature was reached, the flow of Ar or Ar/H_2 was stopped and the main-drain path was opened to bring the inside of the quartz tube to vacuum. The vapor of ethanol was supplied from the temperature-controlled reservoir so that the pressure measured at just before the entrance of the quartz tube is maintained constant. After the CVD reaction, the ethanol vapor was stopped and the electric furnace was turned off before cooled down to the room temperature with a 100 sccm flow of Ar or Ar/H_2.

Thereby obtained sample were analyzed with Raman scattering analysis, FE-SEM and TEM observations, and/or TG analysis depending on the type of produced sample. Raman scattering was measured with Chromex 501is and Andor Technology DV401-FI for the spectrometer and CCD system, respectively, with an optical system of Seki Technotron Corp. STR250. We used Hitachi S-900 and JEOL 2000-EX for FE-SEM and TEM, respectively. TGA was performed with Seiko Instruments Inc. Exter 6000 and TG/DTA 630.

3. Generation of SWNTs from alcohol on USY-zeolite support powder

In order for the efficient production of large amount of SWNTs, we have employed the catalytic metal supported with zeolite powder based on the recipe in Refs. [20, 21]. In brief, iron acetate $(CH_3CO_2)_2Fe$ and cobalt acetate $(CH_3CO_2)_2Co\text{-}4H_2O$ were mixed with typically 1 g of USY-type zeolite powder (Tosoh, HSZ-390HUA, over 99 % SiO_2) so that each metallic weight was 2.5 wt% over the

product powder. The mixture was then dissolved and sonicated in ethanol (typically 20 ml) for 1 h, and dried at 80 °C with occasional sonication to form yellow-brown colored catalyst. The well-dried catalyst was grained in a mortar into a fine powder.

Figure 2 shows a typical TEM image of our 'as-grown' SWNTs produced under the conditions of 800 °C, 5 Torr, and 60 min for the temperature, ethanol vapor pressure, and exposure time during the CVD reaction, respectively, and Ar was used during the heating-up of the electric furnace. As a typical character of as-grown SWNTs synthesized by the alcohol CCVD method [16, 17], there found no metal particles among the bundles of SWNTs and almost no amorphous carbons adhered on the tube walls. Furthermore, no multi-walled carbon nanotubes (MWNTs) were observed in the sample shown in Fig. 2.

Figure 3 shows the Raman scattering spectra for the radial breathing mode (RBM) of SWNTs obtained with 488, 514.5, and 633 nm excitations. The Kataura plot [22] calculated with the condition of $\gamma_0 = 2.9$ eV, $a_{cc} = 0.144$ nm [23] was attached in the top panel, where open and solid circles respectively denote the metallic and semiconducting SWNTs of particular chirality that can resonant with the incident laser of corresponding energy. The sample investigated in Fig. 3 was synthesized under the conditions of 800 °C, 10 Torr, and 10 min for the reaction temperature, pressure, and time during CVD process, respectively. Ar was flowed in the heating-up of the electric furnace. From the location of the RBM peaks the diameter distribution of SWNTs is estimated using a relationship '$d = 248 / \upsilon$' [24] where d (nm) is diameter of a SWNT and υ (cm^{-1}) is the RBM frequency. From Fig. 3, it is shown that the examined SWNTs grown on the zeolite catalytic powder ranges between 0.8 - 1.5 nm containing both metallic and semiconducting SWNTs. The CVD temperature dependence of RBM peaks or diameter distribution for the same sample was presented in Ref. [16], with exhibiting RBM peaks (i.e. identification of SWNT existence) even in the lower temperature synthesis at 550 °C. We have observed that the diameter distribution increases as the reaction temperature became higher. This could be caused by the instability of thinner nanotubes under higher temperature environment, as well as by the sintering of catalytic metals to grow into larger particles.

The TGA (thermo-gravimetric analysis) is an effective tool not only for the estimation of SWNT yield over the produced blackened catalytic powder, but also for the evaluation of the product quality [25-29]. It is often observed that condition of the specimen (e.g. degree of defects or amount of

metallic impurity) largely affects the decomposition temperature of SWNTs [25-28], so caution must be taken in the assignment of the decomposition range of SWNTs. Since it is known that the burning temperature of purified and annealed SWNTs produced by laser-furnace [26] and HiPco [27, 28] techniques are in the range of 500 - 700 °C, this temperature range was assigned for SWNTs because our specimen, as seen in Fig. 2, contains no metallic particle among the SWNTs and tube wall is sufficiently clean (i.e. not covered with amorphous products). Namely, we defined the yield of SWNTs as a ratio of weight loss between 500 and 700 °C to the weight remained at 1000 °C that correspond to the initial weight of catalytic support and metals. Fig. 4 shows the curves of TG and its derivative DTG when the specimen was heated with a heating-up rate of 5 °C/min in a 100 sccm flow of air. All the SWNT samples here were produced under the conditions of 850 °C and 10 Torr for reaction temperature and ethanol vapor pressure during the CVD process, and Ar/H_2 (3% H_2) were supplied during the heating-up of the electric furnace. Very small weight gain around 300 °C was observed due to the oxidation of metal impurities. The slight weight loss around 300 - 500 °C is due to amorphous carbon [25] and subsequent weight loss strongly depends on the CVD time is attributed to the burning of SWNTs, as stated above. Alvarez et al. [13] pointed out that some types of multi-walled carbon product also burn in the higher temperature region; however, the absence of these multi-walled carbons in our samples had been confirmed by TEM observations. Since the amount of amorphous carbon is sufficiently low from TG curves, the high quality of the SWNTs produced by proposed method is again confirmed.

The time progress of SWNT yield is plotted in Fig. 5 where Ar or Ar/H_2 (3% H_2) were employed during the heating-up of the electric furnace in the CVD process. For type of employed gases during the heating, the optimum reaction temperature to assure the best quality is slightly different and they are 800 and 850 °C for the cases of Ar and Ar/H_2, respectively [17]. From this comparison, the effect of reduction by H_2 on the improvement of SWNT yield is apparent. At the best CVD condition of '850 ºC, 10 Torr, Ar/H_2' presented in Fig. 5, the SWNT yield reached more than 40 wt% over the catalytic powder within the CVD time of 120 minutes. This corresponds to more than 800 wt% yield over the catalytic metal because the total metallic concentration in the powder was 5 wt% [17]. Furthermore, our results except for very early stage of reaction indicate the linear increase of the SWNT yield at least in the tested range of CVD time. This is different from the previous reports [8, 9, 14] where nearly 1/2 power-based

slowing down of the yield with reaction time is observed. Hafner et al. [8] attributed this to the decrease of the diffusion rate of carbon feedstock molecule through the thickened layer of SWNTs, while Cassell et al. [9] further suggested the possibilities of pore clogging of the support porous material and catalyst poisoning caused by the growth of SWNTs and amorphous carbons.

The reason why alcohols were much better carbon sources for SWNTs than hydrocarbons is explained by the role of decomposed oxygen radical on the metal catalyst surface. We ascribe the absence of amorphous carbon to an oxygen atom from ethanol molecule, which could selectively oxidize carbon atoms with dangling bonds (i.e. candidate of amorphous carbon) into the form of more stable specie such as CO. Since the selection of SWNTs is made through this etching reaction rather than the conventional selection based on higher temperature stability, the high-quality SWNTs can be generated at lower temperature.

4. Generation of SWNTs from alcohol on solid substrate

Relevant to the desired application of SWNTs to the electronic components and devices, it is crucially important to establish a fundamental technique to incorporate SWNTs into silicon or other basic solid-material based systems. So far, several attempts have been made to synthesize SWNTs on silicon surface [30-35]. Since the employed CVD temperature is rather high (900 - 1000 °C) in these studies, the catalytic metals could react with silicon to form a metal silicide, leading to a significant deterioration of catalytic functions [36]. Successful synthesis of SWNTs only occurred when some support materials such as alumina/silica [30-32] or preliminarily deposited buffering underlayer [33, 36] were employed in order to prevent the silicide formation, whose possibility increases with the CVD temperature. In order for the aforementioned applications, direct mounting of catalytic metals on the silicon substrate is strongly desired. In attempting to achieve this object, we have developed a technique of synthesizing SWNTs directly on the surface of Si and quartz substrates without any intermediating support or underlayer materials [18]. This method does not employ conventional deposition/sputtering technique in mounting of catalytic metals on the surface of substrate, but uniquely employed an easy and costless liquid-based ‘dip-coat’ technique where a piece of the substrates were vertically drawn-up from metal acetate solution at a constant speed: This technique, when combined with our low temperature ACCVD process [16, 17],

does not necessitates any support or underlayer materials.

The brief description of the procedure of our dip-coat process is as follows: First, molybdenum acetate $(CH_3COOH)_2$ Mo and cobalt acetate $(CH_3COOH)_2$ Co-$4H_2O$ were dissolved into ethanol so that the weight concentration of each metal was 0.01 wt% and sonicated for 2 h. A piece of silicon or quartz substrate was vertically suspended in the metal acetate solution with its upper edge held by a small clip connected to a nylon fishing line. After 10 minutes submergence, the piece was drawn up from the acetate solution at a constant pull-up speed of 4 cm/min and dried in air at 400 °C to convert metallic acetate into metal oxides. In the CVD process, Ar/H_2 (3% H_2) were supplied during the heating-up of an electric furnace to reduce the metal oxides for retrieving the catalytic function. With the foregoing methodology, the direct synthesis of high-quality SWNTs on the Si wafer surface has so far been confirmed in the temperature range between 650 and 850 °C [18]. Especially the CVD reaction temperature below 750 °C is effective, regardless of the thickness of natural oxidation layer of Si wafer, to circumvent the silicide formation that is a major problem in the conventional high-temperature CVD techniques [36].

One feature of the proposed technique lies in its ability of producing macroscopic amount of SWNTs on the substrate. Fig. 6 shows the SEM image of a quartz substrate (thickness 0.5 mm, both sides optically polished) taken from a tilted angle including broken cross-section of the substrate. The CVD was performed at 800 °C for 1 h using Ar/H_2 (3% H_2) in the heating-up in the CVD process. The substrate was blackened and a uniform ‘mat’ of SWNTs with a thickness of a few hundred nanometers was formed on the both sides of the quartz substrate. Since the optical properties of thereby produced ‘as-grown’ SWNT mat is readily measured [18], this technique is considered to open-up a new application of SWNTs toward novel optical devices such as optical switches utilizing bleached absorption of SWNTs [37].

In aiming at more spatially controlled growth of SWNTs, there are several studies in which the geometrical characteristics of mesoporous silica (MPS) were utilized in the synthesis of carbon nanotubes [38-42]: However, their products were multi-walled nanotubes except Huang et al. [42] who showed no evidence on the type of the product. Since the most of fascinating physical properties of carbon nanotubes including the metal-semiconducting duality is of single-walled ones, the establishment of SWNT synthesis technique from the MPS thin film has been desired for the controlled growth. We have

achieved this in Ref. [19] employing a thin film of SBA-16 [43] combined with the alcohol CCVD technique. The uniqueness of proposed technique lies in our ‘post’ metallic mounting approach where the catalytic metals were loaded inside/on the surface of MPS thin film after the formation of MPS structure. Conventionally, all the past reports [38-42] mixed the catalytic metal species at the stage of preparation of sol-gel solution i.e. before the formation of MPS structure. However, as pointed out by Zheng et al. [40], such approach could cause the deformation of MPS structure caused by the metallic atoms included within the silica frameworks. The soundness of our MPS structure assured by the post-loading of catalytic metal as well as relatively low synthesis temperature (750 °C) by the ACCVD method could contribute to the synthesis of the high-purity SWNTs.

The Raman spectra of SWNTs grown on the foregoing bases (USY-zeolite, Si, quartz, and MPS) were compared in Fig. 7. The excitation laser wavelength was 488 nm for all cases. Although there are differences in the diameter distributions depending on the types of employed substrates, RBM peaks were clearly observed and the ratios of G/D peaks were sufficiently high for all the cases. Authors believe that the foregoing techniques synthesizing high-quality SWNTs on various types of substrates could make a partial contribution to the development of SWNT-based innovative devices incorporated in the solid surfaces.

5. Molecular dynamics simulation

The formation mechanism in the laser-furnace method and CCVD method should be considerably different at least at the nucleation stage of SWNTs. In the former method, carbon atoms and catalytic metal atoms are vaporized at the same time by the intense laser ablation. In the latter, the catalytic metal clusters are present before the assembly of carbon atoms. Hence, 2 different simulation conditions, ‘co-vaporization’ and ‘CCVD’ are compared below. The Brenner potential [44] in its simplified form [45, 46] was used for the carbon-carbon interaction. The metal-carbon potential was constructed with the covalent term based on the coordination number of metal atom and the Coulomb term due to the charge transfer from metal to carbon cluster [47].

Generation conditions of SWNTs by the laser-furnace or by the arc discharge techniques are almost the same as for fullerene and endohedral metallofullerene except for the doped metal species.

Hence, the same molecular dynamics simulation condition as for our previous empty fullerene [45, 46] and for endohedral metallofullerene [47] except for the catalytic Ni atoms was employed. As the initial condition, the completely random vapor mixture of 2500 carbon and 25 Ni atoms were allocated in a 58.5 nm cubic fully-periodic simulation cell [48, 49]. After 6 ns molecular dynamics calculation, many relatively large clusters up to about 200 carbon atoms and a few metal atoms were observed. Carbon clusters tended to be spherical random cage structure with a few metal atoms at around the defect vacancy, which prevented the cage structure from the complete closure. These imperfect carbon cage structures with several metal atoms outside were partially confirmed by the FT-ICR reaction experiments of laser vaporized clusters [50]. In the later stage, the periodic cell size was slowly reduced to enhance the collision events in order to further accelerate the simulation. A large tubular structure was obtained after coalescence of clusters. Ni atoms were slowly assembling to form Ni clusters, and they were diffusing around until finding the most stable position at the hemi-half-fullerene cap area. Given the enough time for the diffusion of metal atoms and network annealing, it is expected that the structure becomes a straight SWNT with metal clusters at each end.

The ‘CCVD’ molecular dynamics simulations started from a Ni cluster and randomly distributed carbon atoms, where hydrogen or oxygen atoms in the carbon-source molecule were not explicitly included for the simplicity. We adopted a floated catalyst, as in the case of HiPco process [5, 6], rather than the supported catalyst on a solid surface. Assuming that carbon atoms do not form carbon-carbon bonds until they reach the surface of Ni particle, we introduced a van der Waals potential for repulsion among the vaporized carbon atoms. The chemical reaction process such as a decomposition of carbon source molecule at the surface of the metal cluster was completely neglected in this simplified simulation. Upon arrival of a carbon-containing molecule to the bare metal surface, it was assumed that such reaction would immediately take place. Hence, such reaction barrier was implicitly included in the net flux of carbon-containing molecules. As the initial metal cluster size, Ni_{32}, Ni_{108} and Ni_{256} corresponding to about 0.8 nm, 1.3 nm and 1.6 nm in diameters, respectively, were prepared as shown in Fig. 8. In addition to the metal cluster, completely random vapor mixture of carbon-containing molecules was allocated in 20 nm cubic periodic cell.

Fig. 9 shows an example of the nucleation process starting from Ni_{108}. At an earlier stage of the

simulation, all carbon atoms were absorbed in the metal cluster. When saturated, hexagonal carbon networks were observed inside the metal-carbon binary cluster. Depending on the initial Ni cluster size and on temperature, the formation of various nanotube cap structures was demonstrated with the continuous supply of carbon [51]. As shown in Fig. 10, observed typical formation process of nanotube cap is as following. An annular graphitic sheet grows up from circumferential edge of pseudo-crystal domain of the metal-carbon cluster and then the open sheet makes a closure to form a cap structure. This formation process is considerably different from the yarmulke model [4].

6. Conclusion

We have developed a method of producing high-quality SWNTs adopting alcohol as a carbon feedstock. This method presents a good performance not only for the mass-production of SWNTs, but also for the direct synthesis of SWNTs on non-metallic substrates such as silicon and quartz. As for the mass production of SWNTs, this method can achieve the yield of more than 40 wt % over the initial weight of catalytic powder, i.e. USY-zeolite supporting 5 wt % catalytic metals, within the CVD reaction of 120 min. The TEM, Raman, and TG analyses performed on the as-prepared sample revealed that the produced sample have sufficiently high quality almost free from the contaminations such as amorphous carbon or metal impurities. When combined with the proposed dip-coat approach for the loading of catalytic metal, the alcohol CCVD method produced high-quality SWNTs directly on the surface of silicon and quartz surfaces without necessitating any support/underlayer materials. This is attributed to our considerably low CVD temperature (i.e. 650 to 800 ºC) that effectively suppresses the formation of metal silicide. In order to investigate the mechanism of SWNT nucleation, we performed several molecular dynamics simulations for the CCVD situations. We have successfully simulated the formation of carbon caps and discussed an initial nucleation mechanism of a SWNT. Common future works include an enhancement of quality/quantity of the produced SWNTs and a development of a control technique of their diameter/chilarity, both would be achieved through further experimental and numerical studies.

Acknowledgements

The authors thank Mr. H. Tsunakawa (The University of Tokyo) for his assistance in TEM observations and Mr. T. Sugawara (The University of Tokyo) for his technical advices in FE-SEM observations. Part of this work was supported by KAKENHI #12450082 and 13555050 from JSPS, and #13GS0019 from MEXT.

References

[1] S. Iijima, T. Ichihashi, Nature 363, 603 (1993).

[2] A. Thess, R. Lee, P. Nikolaev, H. Dai, P. Petit, J. Robert, C. Xu, Y. H. Lee, S. G. Kim, A. G. Rinzler, D. T. Colbert, G. E. Scuseria, D. Tománek, J. E. Fischer, R. E. Smalley, Science 273, 483 (1996).

[3] C. Journet, W. K. Maser, P. Bernier, A. Loiseau, M. L. de la Chapelle, S. Lefrant, P. Deniard, R. Lee, J. E. Fisher, Nature 388, 756 (1997).

[4] H. Dai, A. G. Rinzler, P. Nikolaev, A. Thess, D. T. Colbert, R. E. Smalley, Chem. Phys. Lett. 260, 471 (1996).

[5] P. Nikolaev, M. J. Bronikowski, R. K. Bradley, F. Rohmund, D. T. Colbert, K. A. Smith, R. E. Smalley, Chem. Phys. Lett. 313, 91 (1999).

[6] M. J. Bronikowski, P. A. Willis, D. T. Colbert, K. A. Smith, R. E. Smalley, J. Vac. Sci. Technol. A 19, 1800 (2001).

[7] J. Kong, A. M. Cassell, H. Dai, Chem. Phys. Lett. 292, 567 (1998).

[8] J. H. Hafner, M. J. Bronikowski, B. R. Azamian, P. Nikolaev, A. G. Rinzler, D. T. Colbert, K. A. Smith, R. E. Smalley, Chem. Phys. Lett. 296, 195 (1998).

[9] A. M. Cassell, J. A. Raymakers, J. Kong, H. Dai, J. Phys. Chem. B 103, 6484 (1999).

[10] B. Kitiyanan, W. E. Alvarez, J. H. Harwell, D. E. Resasco, Chem. Phys. Lett. 317, 497 (2000).

[11] M. Su, B. Zheng, J. Liu, Chem. Phys. Lett. 322, 321 (2000).

[12] J.-F. Colomer, J.-M. Benoit, C. Stephan, S. Lefrant, G. Van Tendeloo, J. B. Nagy, Chem. Phys. Lett. 345, 11 (2001).

[13] W. E. Alvarez, B. Kitiyanan, A. Borgna, D. E. Resasco, Carbon 39, 547 (2001).

[14] B. Zheng, Y. Li, J. Liu, Appl. Phys. A 74, 345 (2002).

[15] W. E. Alvarez, F. Pompeo, J. E. Herrera, L. Balzano, D. E. Resasco, Chem. Mater. 14, 1853 (2002).

[16] S. Maruyama, R. Kojima, Y. Miyauchi, S. Chiashi, M. Kohno, Chem. Phys. Lett. 360, 229 (2002).

[17] Y. Murakami, Y. Miyauchi, S. Chiashi, S. Maruyama, Chem. Phys. Lett. 374, 53 (2003).

[18] Y. Murakami, Y. Miyauchi, S. Chiashi, S. Maruyama, Chem. Phys. Lett. 377, 49 (2003).

[19] Y. Murakami, S. Yamakita, T. Okubo, S. Maruyama, Chem. Phys. Lett. 375, 393 (2003).

[20] K. Mukhopadhyay, A. Koshio, N. Tanaka, H. Shinohara, Jpn. J. Appl. Phys. 37, L1257 (1998).

[21] K. Mukhopadhyay, A. Koshio, T. Sugai, N. Tanaka, H. Shinohara, Z. Konya, J. B. Nagy, Chem. Phys. Lett. 303, 117 (1999).

[22] H. Kataura, Y. Kumazawa, Y. Maniwa, I. Umezu, S. Suzuki, Y. Ohtsuka, Y. Achiba, Synth. Met. 103, 2555 (1999).

[23] R. Saito, G. Dresselhaus, M. S. Dresselhaus, Phys. Rev. B 61, 2981 (2000).

[24] A. Jorio, R. Saito, J. H. Hafner, C. M. Lieber, M. Hunter, T. McClure, G. Dresselhaus, M. S. Dresselhaus, Phys. Rev. Lett. 86, 1118 (2001).

[25] E. Mizoguti, F. Nihey, M. Yudasaka, S. Iijima, T. Ichihashi, K. Nakamura, Chem. Phys. Lett. 321, 297 (2000).

[26] I. W. Chiang, B. E. Brinson, R. E. Smalley, J. L. Margrave, R. H. Hauge, J. Phys. Chem. B 105, 1157 (2001).

[27] W. Zhou, Y. H. Ooi, R. Russo, P. Papanek, D. E. Luzzi, J. E. Fischer, M. J. Bronikowski, P. A. Willis, R. E. Smalley, Chem. Phys. Lett. 350, 6 (2001).

[28] M. Chike, J. Li, B. Chen, A. Cassell, L. Delzeit, J. Han, M. Mayyappan, Chem. Phys. Lett. 365, 69 (2002).

[29] M. Zhang, M. Yudasaka, A. Koshio, S. Iijima, Chem. Phys. Lett. 364, 420 (2002).

[30] J. Kong, H. T. Soh, A. M. Cassell, C. F. Quate, H. Dai, Nature 395, 878 (1998).

[31] A. M. Cassell, N. R. Franklin, T. W. Tombler, E. M. Chan, J. Han, H. Dai, J. Am. Chem. Soc. 121, 7975 (1999).

[32] N. R. Franklin, Y. Li, R. J. Chen, A. Javey, H. Dai, Appl. Phys. Lett. 79, 4571 (2001).

[33] L. Delzeit, B. Chen, A. Cassell, R. Stevens, C. Nguyen, M. Meyyappan, Chem. Phys. Lett. 348, 368 (2001).

[34] O. A. Nerushev, R. E. Morjan, D. I. Ostrovskii, M. Sveningsson, M. Jonsson, F. Rohmund, E. E. B. Campbell, Physica B 323, 51 (2002).

[35] Y. J. Yoon, J. C. Bae, H. K. Baik, S. Cho, S. Lee, K. M. Song, N. S. Myung, Chem. Phys. Lett. 366, 109 (2002).

[36] T. de los Arcos, F. Vonau, M. G. Garnier, V. Thommen, H.-G. Boyen, P. Oelhafen, M. Duggelin, D. Mathis, R. Guggenheim, Appl. Phys. Lett. 80, 2383 (2002).

[37] S. Tatsuura, M. Furuki, Y. Sato, I. Iwasa, M. Tian, H. Mitsu, Adv. Mater. 15, 534 (2003).

[38] A. M. Cassell, S. Verma, L. Delzeit, M. Meyyappan, J. Han, Langmuir 17, 260 (2001).

[39] G. Zheng, H. Zhu, Q. Luo, Y. Zhou, D. Zhao, Chem. Mater. 13, 2240 (2001).

[40] F. Zheng, L. Liang, Y. Gao, J. H. Sukamto, C. L. Aardahl, Nano Lett. 2, 729 (2002).

[41] N. Petkov, S. Mintova, K. Karaghiosoff, T. Bein, Mat. Sci. Eng. C 23, 145 (2003).

[42] L. Huang, S. J. Wind, S. P. O'Brien, Nano Lett. 3, 299 (2003).

[43] D. Zhao, P. Yang, N. Melosh, J. Feng, B. F. Chmelka, G. D. Stucky, Adv. Mater. 10, 1380 (1998).

[44] D. W. Brenner, Phys. Rev. B 42, 9458 (1990).

[45] Y. Yamaguchi, S. Maruyama, Chem. Phys. Lett. 286, 336 (1998).

[46] S. Maruyama, Y. Yamaguchi, Chem. Phys. Lett. 286, 343 (1998).

[47] Y. Yamaguchi, S. Maruyama, Euro. Phys. J. D 9, 385 (1999).

[48] Y. Shibuta, S. Maruyama, Physica B 323, 187 (2002).

[49] S. Maruyama, Y. Shibuta, Mol. Cryst. Liq. Cryst. 387, 87 (2002).

[50] M. Kohno, S. Inoue, R. Kojima, S. Chiashi, S. Maruyama, Physica B 323, 272 (2002).

[51] Y. Shibuta, S. Maruyama, Chem. Phys. Lett., to be submitted.

Captions to Figures

Fig. 1. Schematic description of experimental apparatus for the alcohol CCVD.

Fig. 2. A TEM image of 'as-grown' SWNTs synthesized under the conditions of 800 °C, 5 Torr, and 1 h for the temperature, ethanol vapor pressure, and reaction time during CVD process. Ar was used while heating-up of the electric furnace. Note the absence of metallic impurities and multi-walled carbon products.

Fig. 3.Raman spectra of RBM of SWNTs synthesized under the conditions of 800 °C, 10 Torr and 10 min for the temperature, ethanol pressure, and time during CVD process, respectively. Ar was used while heating-up of the electric furnace. The spectra were taken with 3 different laser excitations, 488, 514.5, 633 nm. In the bottom was the Kataura plot for the corresponding abscissa range, where open and solid circles represents the metal and semiconducting SWNTs of particular chirality with corresponding energy gaps.

Fig. 4. TGA curves of as-grown blackened powder for the CVD reaction times of 10, 60, and 120 minutes and its derivative DTG (bottom). The temperature and ethanol pressure during CVD were 850 °C and 10 Torr, respectively. During the heating-up of the electric furnace, Ar/H_2 (3% H_2) was supplied for the metal reduction.

Fig. 5 SWNT yield progression with CVD time for the sample produced under the conditions of '850 °C, 10 Torr, Ar/H2' (circle) and '800 °C, 10 Torr, Ar' (square) for the CVD temperature, ethanol pressure, and the gas used while the electronic furnace was heated up, respectively.

Fig. 6 FE-SEM image of SWNTs directly synthesized on a quartz substrate taken from tilted angle including broken cross-section of the substrate. The generated mat of SWNTs on the quartz surface has a thickness of a few hundred nanometers. The CVD condition for this sample was 800 °C, 10 Torr, 1 h for the temperature, ethanol vapor pressure, and reaction time during CVD process, respectively. Ar/H_2 were flowed during the heating-up of the electric furnace.

Fig. 7 Raman spectra of SWNTs grown on USY-zeolite, Si and quartz substrates, and MPS thin film coated on Si wafer. Excitation laser used was 488 nm for all cases. The high wave number range (right panel) indicates all of the produced SWNTs have sufficient high quality according to the G/D ratio of the spectra. The magnification of lower wave number region (left panel) exhibits their RBM spectra, from which the diameter distribution for each case is estimated.

Fig. 8. Initial condition of growth simulation for CCVD method. Completely random vapor mixture of 500 carbon-containing molecules and a nickel cluster were allocated in 200 Å cubic periodic cell.

Fig. 9. Snapshots of metal-catalyzed growth process of the cap structure after 130 ns molecular dynamics calculation at 2500K for Ni_{108}. Spheres represent nickel atoms. All carbon atoms are not shown for clarity. Arrows indicate the supply of carbon atoms from expose metal surface.

Fig. 10. An example of nucleation process of SWNT cap from a Ni cluster. Annular graphitic sheet grown up from circumferential edge of pseudo-crystal domain of the metal-carbon cluster.

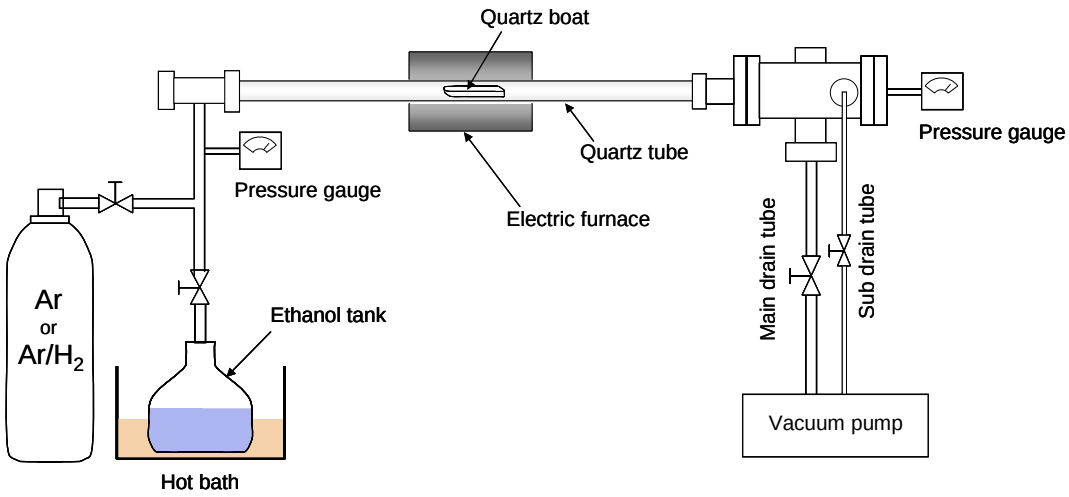
Quartz boat
Quartz tube
Pressure gauge
Pressure gauge
Electric furnace
Main drain tube
Sub drain tube
Ar
or
Ar/H2
Ethanol tank
Vacuum pump
Hot bath

Fig. 1

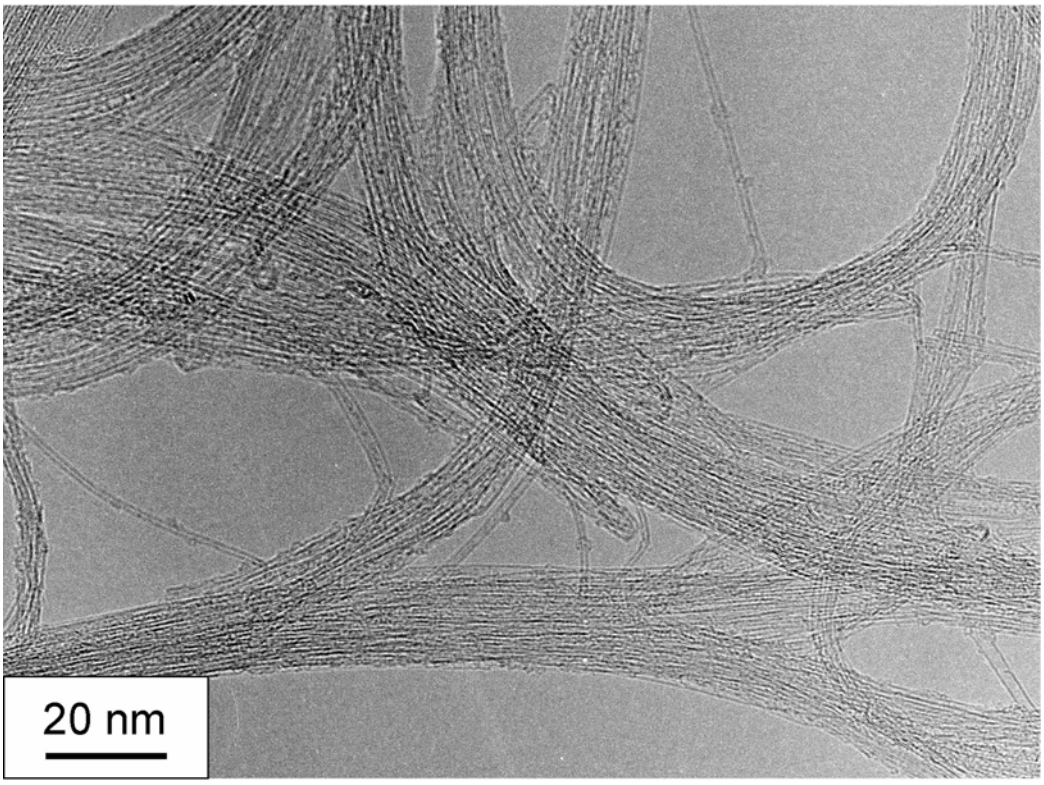

Fig. 2

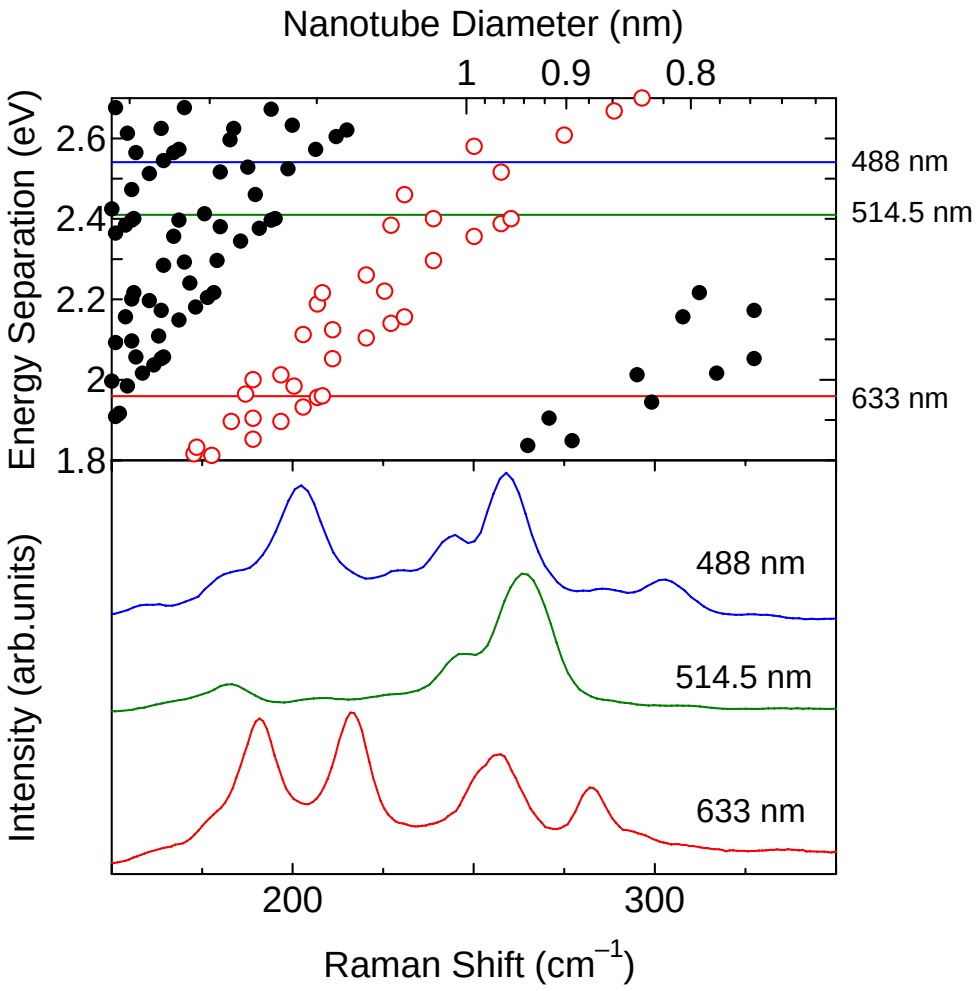
Nanotube Diameter (nm)
1
0.9
0.8
Energy Separation (eV)
2.6
2.4
2.2
2
1.8
488 nm
514.5 nm
633 nm
Intensity (arb.units)
488 nm
514.5 nm
633 nm
200
300
Raman Shift (cm^{-1})

Fig. 3

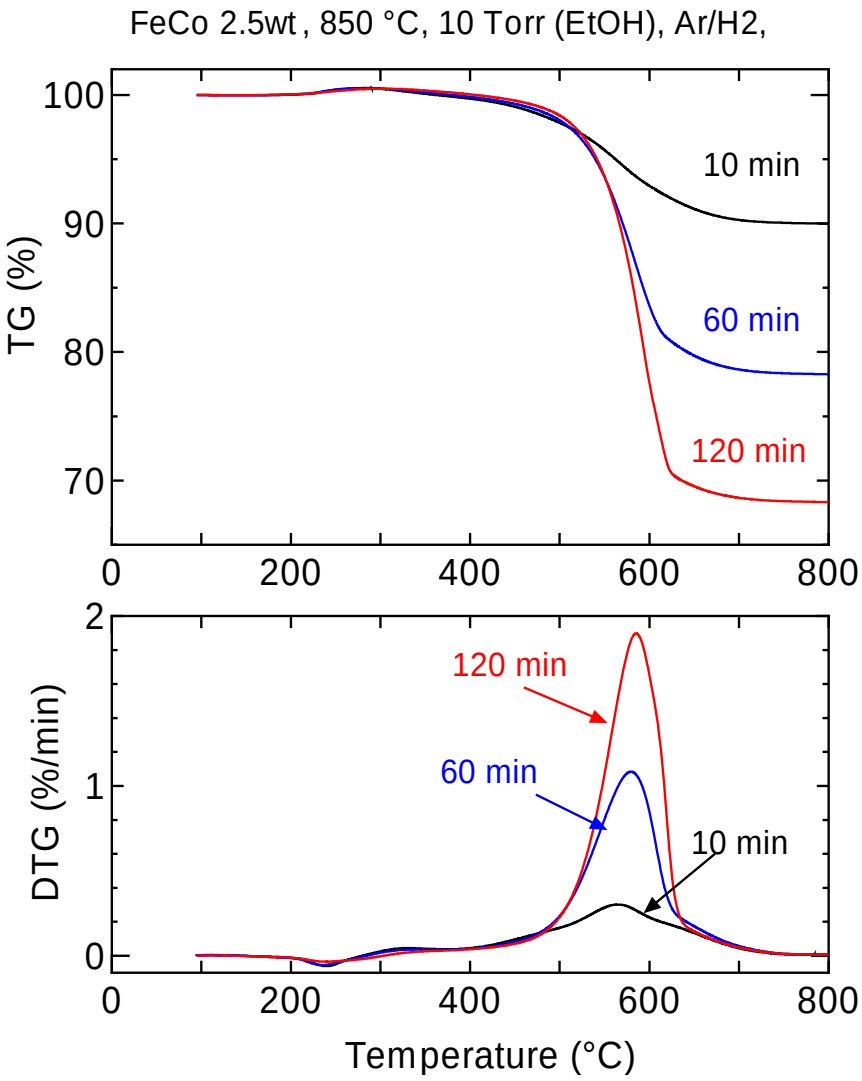
FeCo 2.5wt , 850 °C, 10 Torr (EtOH), Ar/H2,
TG (%)
100
90
80
70
10 min
60 min
120 min
0
200
400
600
800
DTG (%/min)
2
1
0
120 min
60 min
10 min
Temperature (°C)

Fig. 4

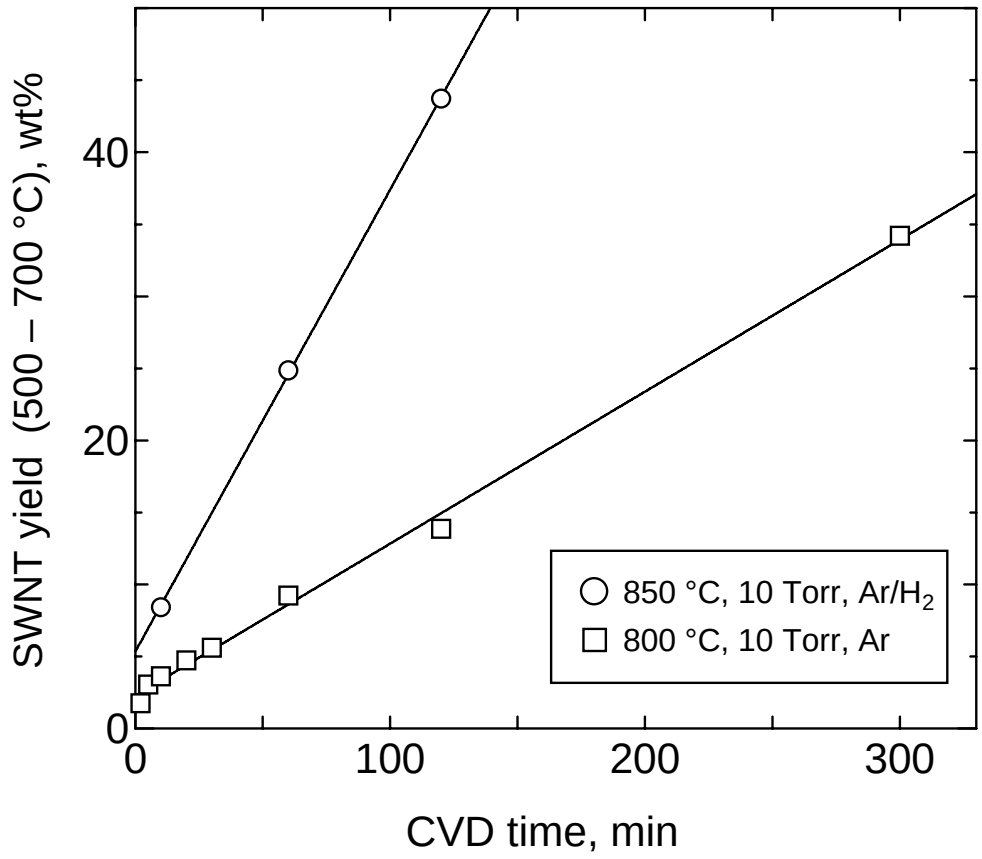
SWNT yield (500 – 700 °C), wt%
0
20
40
0
100
200
300
CVD time, min
850 °C, 10 Torr, Ar/H2
800 °C, 10 Torr, Ar

Fig. 5

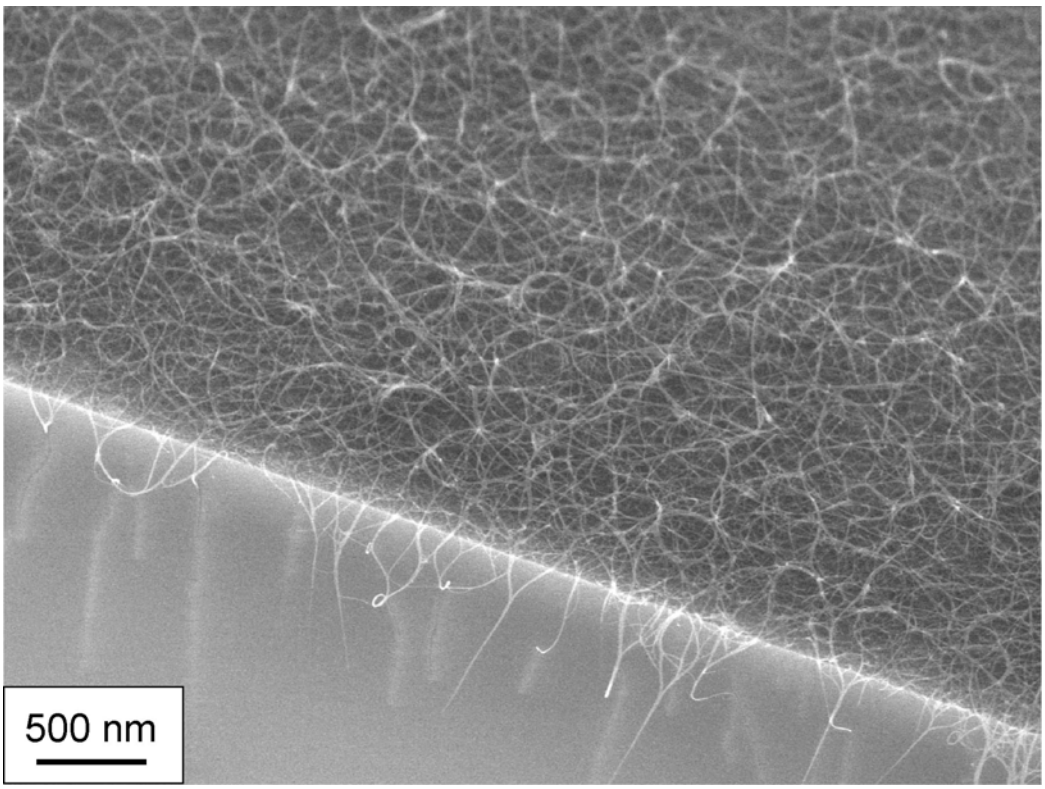

Fig. 6

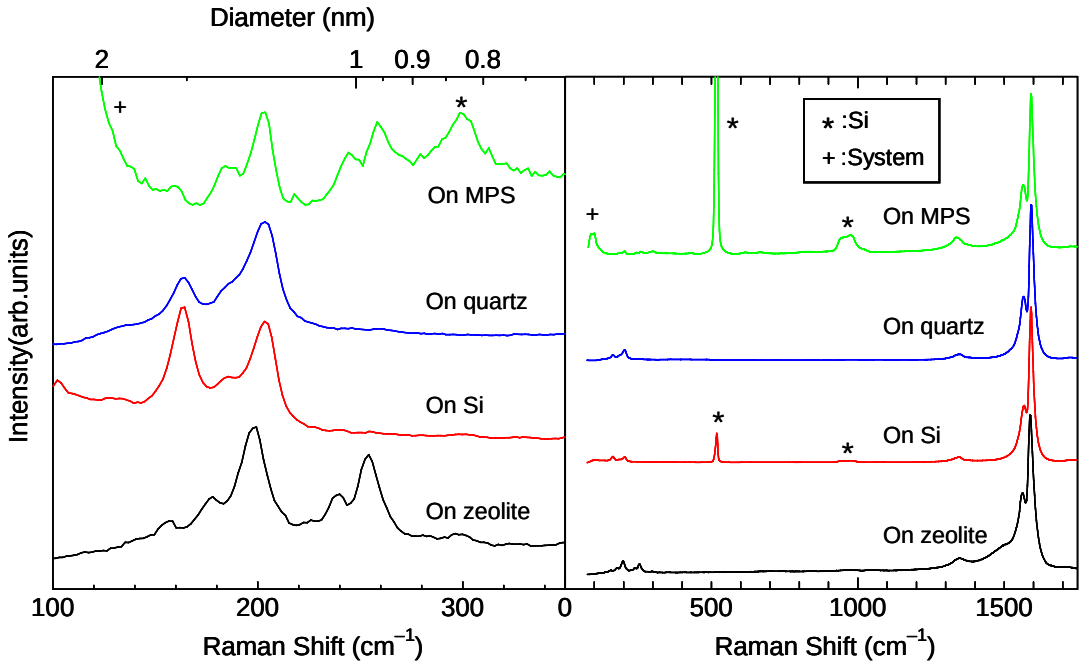
Diameter (nm)
2
1
0.9
0.8
Intensity(arb.units)
On MPS
On quartz
On Si
On zeolite
100
200
300
0
Raman Shift (cm^{-1})
* :Si
+ :System
500
1000
1500
Raman Shift (cm^{-1})

Fig. 7

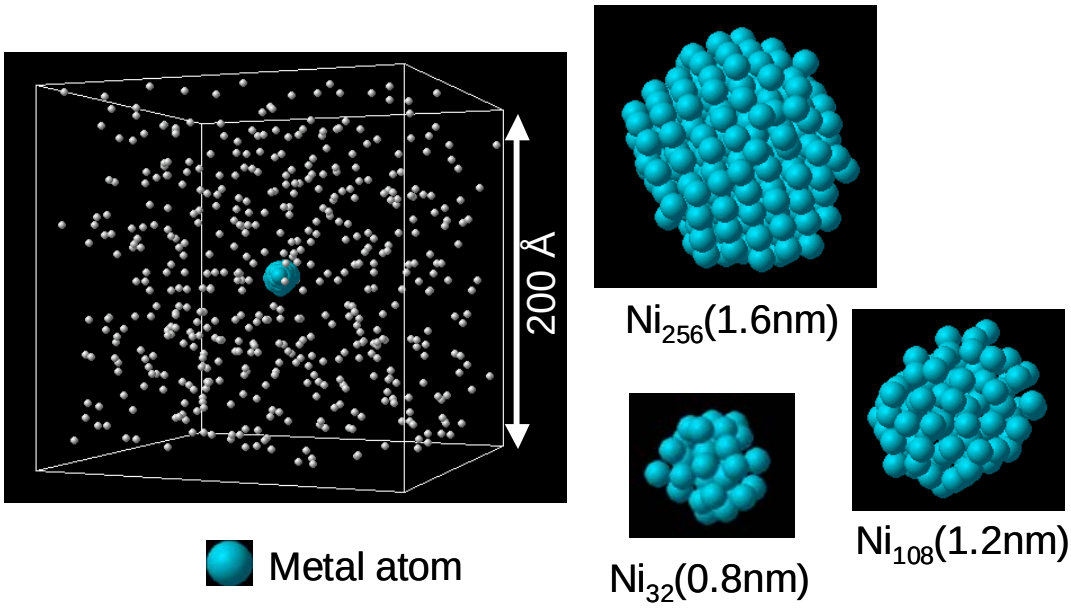

Fig. 8

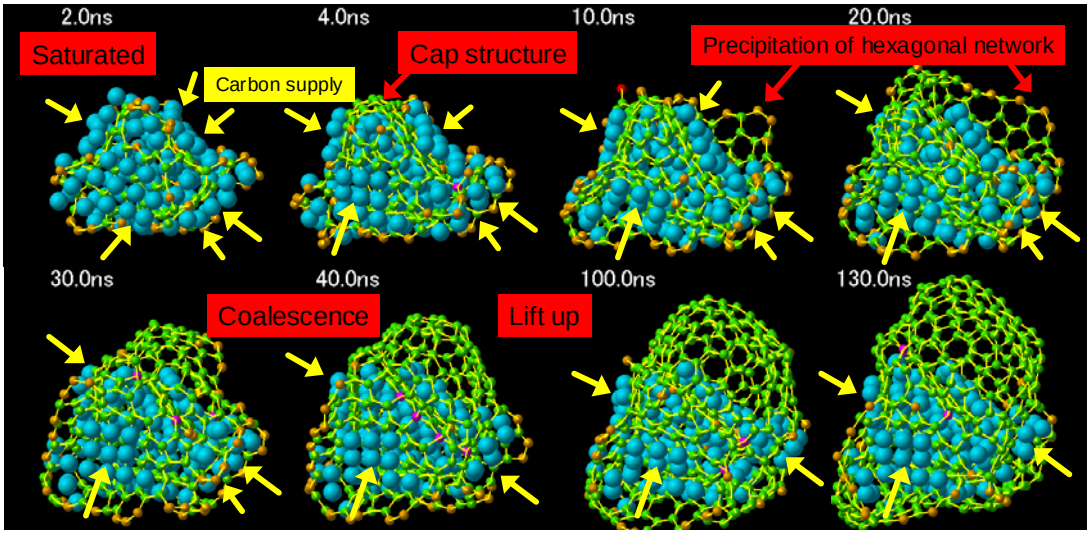
2.0ns
4.0ns
10.0ns
20.0ns
Saturated
Carbon supply
Cap structure
Precipitation of hexagonal network
30.0ns
40.0ns
100.0ns
130.0ns
Coalescence
Lift up

Fig. 9

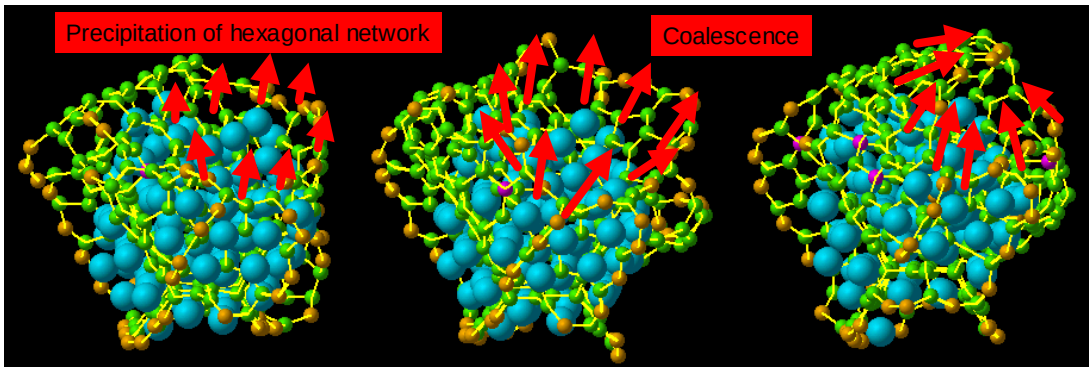

Fig. 10